The three-dimensional solution structure of a constrained peptidomimetic in water and in chloroform Observation of solvent induced hydrophobic cluster

Min S. Lee[a,b,*], Benjamin Gardner[a], Michael Kahn[a,b], Hiroshi Nakanishi[a,b,*]

[a]*Molecumetics, Bellevue, WA 98005, USA*
[b]*Department of Pathobiology, SC-38, University of Washington, Seattle, WA 98195, USA*

Received 14 November 1994; revised version received 19 December 1994

Abstract **A large number of protein–protein interactions involve turn or loop regions. The excised linear peptides from these regions reveal complex conformational averaging. To circumvent this motional averaging and to stabilize the β-turn conformation, extensive effort has been devoted to the design of constrained peptidomimetics. Here, we report the three-dimensional solution structure of a 12-membered cyclic peptidomimetic. The structures were calculated from NMR studies performed in chloroform and in water at 263 and 278K, respectively. This 12-membered cyclic scaffolding is part of a program to design and to construct conformationally stable β-turn peptidomimetics. The impact of the surrounding environment on the conformation of this constrained peptidomimetic is discussed. The general structural features of the cyclic mimetic are retained in both environments; however, the formation of a hydrophobic patch in the aqueous solvent is evident.**

Key words: Peptidomimetic; Hydrophobic cluster; Solution structure; Nuclear magnetic resonance; Solvent effect

1. Introduction

All physiological processes are directly or indirectly regulated by ligands, peptides, and proteins through their interactions with their cognate carbohydrate, protein, or nucleic acid receptors. Many interactions are dominated by only a small interface for their specific recognition and thus require only a few exposed residues. This specificity is the result of a particular spatial arrangement of side chain functionality presented in the context of a helix, reverse turn, or β-sheet scaffolding. A large number of interactions originate from turn or loop regions within the protein. The excised linear peptides from these regions reveal vast and complex conformational averaging in solution. To overcome this averaging, extensive effort has been devoted to the design of constrained peptides and peptide mimetics (peptidomimetics). A number of conformational studies of turns in peptides and peptidomimetics have been performed [1–5]. However, the critical role of the solvent environment and its effect on conformation cannot be neglected when considering structures in solution. The ability to design and to determine a well-defined stable three-dimensional solution structure of a molecule makes an important contribution to our basic understanding of structure, protein folding, and the physiological interactions involving ligands and receptors.

A large array of cyclic peptides have been studied in solution by NMR. However, the vast majority of NMR studies have been performed in non aqueous solvents [6–20]. Many of these solution studies are restricted to conformational analysis based on qualitative NOE data, modeling, and molecular dynamics (MD). In addition, there is minimal experimental evidence of the effect of solvent on the conformational aspects of constrained peptidomimetics. Here, we report the three-dimensional solution structure of a cyclic peptidomimetic as determined by NMR in water and in chloroform. The impact of the surrounding environment on the conformation of this constrained peptidomimetic is discussed.

2. Materials and methods

2.1. Sample preparation

The constrained peptidomimetics **1** and **2** (Fig. 1) were synthesized and purified as described previously with modifications for the side chains [21]. The peptide sequence for the mimetic framework is derived from the endogenous opioid pentapeptide, leucine enkephalin (Tyr-Gly-Gly-Phe-Leu) [22]. The sample for NMR spectroscopy was prepared by dissolving the peptidomimetic **1** in 100% ^2H_2O and later the lyophilized ^2H_2O sample was dissolved in 90% ^1H_2O/10% ^2H_2O to give sample concentration of ~5 mM at pH ~3. The pH was measured with a glass electrode and was not corrected for isotope effects. The peptidomimetic **2** was dissolved in $CDCl_3$ at a concentration of ~5 mM.

2.2. Acquisition of NMR spectra

The NMR experiments were performed using a Varian Unity 500 MHz spectrometer. Spectra were recorded at 0.5, 5, 10, and 25°C with the carrier set on the ^1H_2O or residual HOD at 4.96 ppm for the water sample and at −10 and 25°C with the carrier set on the residual $CHCl_3$ at 7.26 ppm for the chloroform sample. The $^3J_{HN\alpha}$ and $^3J_{\alpha\beta}$ coupling constants were obtained directly from the resolved proton resonances in the 1D spectra. Standard pulse sequences and phase cycling schemes were used for the 2QF-COSY [23], ROESY [24], NOESY [25], and jump-and-return NOESY [26] experiments with 32–64 scans per t_1 value and 450–800 t_1 values. Low-power irradiation of the solvent resonance during the relaxation delay of 1.4–1.5 s was used for all experiments in water with the exception of jump and return NOESY. ROE buildup curves were obtained for mixing times of 150, 200, 300, 400, 450, and 600 ms for water sample and 100, 150, 200, 250, and 300 ms for chloroform sample. From the evaluation of the buildup curves, the data from the 200 ms ROESY spectrum was then chosen for the generation of constraints. All 2D spectra were acquired with 2048 complex data points and a spectral width of 5,000–6,250 Hz in F_2 and 4,000–5,000

*Corresponding authors. Molecumetics, 2023 120th Ave., N.E. Ste. 400, Bellevue, WA 98005, USA. Fax: (1) (206) 646 8890.

Abbreviations: NMR, nuclear magnetic resonance; DG, Distance geometry; SA, Simulated annealing; ppm, parts per million; SASA, solvent accessible surface area.

SSDI 0014-5793(95)00007-0

Hz in F_1. Spectra were recorded in the phase-sensitive mode with quadrature detection in the F_1 dimension using the methods of States and Haberkorn [27].

2.3. NMR data processing

All NMR data were transferred to a Silicon Graphics Iris Indigo 2/XZ and processed using the program FELIX (BIOSYM Technologies, Inc.). NOESY, jump and return NOESY, and ROESY spectra were Fourier transformed using a Lorentzian-to-Gaussian weighting function in the F_2 dimension and a shifted sine bell weighting function in the F_1 dimension. For 2QF-COSY data, unshifted sine bell and shifted sine bell weighting functions for F_2 and F_1 dimensions were used, respectively. For spectra recorded in 90% ^1H_2O/10% ^2H_2O, a low frequency-deconvolution was applied to the time domain data prior to Fourier transformation in order to reduce the size of the residual ^1H_2O [28]. The transformed spectra contained 2,048 real points in both dimensions.

2.4. Structure calculation

The ROE cross peaks were assigned and interproton distances were calculated from the cross peak volumes in the ROESY spectra under the rigid body approximation where a single correlation time τ_c was assumed for all interaction vectors. The interproton distances d_{ij} were calculated using

$$d_{ij} = d_{ref} (ROE_{ref}/ROE_{ij})^{-6}$$

where d_{ref} is a known distance between two protons used for calibration and ROE_{ref} is the corresponding cross peak volume. Lower bounds were set to the sum of their van der Waals radii between non-bonded atoms. Upper and lower bounds for the φ and $\chi 1$ dihedral angles were assigned by inspection of the values of the $^3J_{HN\alpha}$ [29] and $^3J_{\alpha\beta}$ [30] coupling constants. Pseudoatoms were used wherever necessary [31]. ROE derived distance constraints, anti-distance constraints (adc) [32], and dihedral angle constraints were used in the structure calculations. The adc were derived from analysis of missing cross peaks, leading to a list of absent distance constraints. In this study, an absent cross peak is attributed to a lower bound or a minimum distance of 4.0 Å for explicit proton distances and 3.0 Å whenever a psuedoatom is involved. In addition, floating chirality for chemically inequivalent β-methylene and methyl group protons were used wherever appropriate. For peptidomimetic **1** in water, 45 ROE distance constraints, 2 dihedral angle constraints, and 193 adc were used as input data for structural calculation. For peptidomimetic **2** in chloroform, 39 ROE, 1 dihedral constraints, and 97 adc were used. Additionally, similar results were obtained when structure calculations were carried out without adc. During DGII/SA and energy minimization, a force constant of 32 kcal/mol·Å^2 was used for the half-parabolic NOE and adc penalty functions.

Distance geometry calculations were carried out using the program DGII (BIOSYM Technologies, Inc., San Diego). The bounds for the inter-atomic distances were smoothed by using triangular inequality and 20 structures were embedded in 4D space, followed by optimization using a simulated annealing protocol with sigmoidal cooling schedule from a maximum temperature of 200 K in 20,000 steps at simulation steps of 2 fs. All peptide bonds were allowed to rotate freely during the optimization to account for the highly strained nature of the small cyclic peptidomimetic. The structures were then energy minimized using DISCOVER class II cff91 force field with NMR constraints.

3. Results and discussion

The NMR studies of **1** and **2** (Fig. 1) were performed in water and in chloroform at 278 and 263 K, respectively. Sequence-specific resonance assignments were made by standard methods from homonuclear two-dimensional spectra [33]. The 12-membered cyclic scaffolding is part of a series in our continuing program to design and to synthesize conformationally stable β-turn peptidomimetics [2,34–36]. The NMR spectra of the constrained mimetics display wide chemical shift dispersion, a characteristic common to a folded protein (Table 1). In particular, the C^α and C^β protons of the Leu residue in water show chemical shifts significantly different from random coil values [37]. The chemical shift difference of 0.28 for C^α and 0.11 and 0.22 ppm for C^β protons for this residue indicate a possible presence of structure and/or interaction with an aromatic residue. The importance of deviation of ^1H NMR chemical shifts from the random-coil values for urea-unfolded 434 repressor [38,39] and denatured BPTI [40] have been implicated in the identity of residual non-random structure. Furthermore, the identity, location, and solution conformation of the structured region in the urea-denatured 434 repressor was guided by the chemical shift data in combination with amide exchange.

In both solvents, we observe a very strong ROE between the C^α protons of Phe and Leu, indicative of a *cis*-peptide bond at the tertiary amide linkage. The ROE between sequential C^α protons is observed only in the 12-membered gem-dimethyl linker containing structure but not in the analogous 10- and 14-membered and 12-membered mono-methyl linker containing cyclic scaffolding (unpublished results; M.S.L, Bolong Cao, Jan Urban, M.K., and H.N.). The other key ROE is the observation of interaction between the Phe and Leu side chains indicating hydrophobic clustering in water. While the chemical shift of the Leu protons differ from that of the random coil shift, the difference in magnitude reflects the averaging with other conformation that give rise to the ROE. Thus, it is not easy to determine the population of one conformer giving rise to one specific ROE. Wüthrich and co-workers [39] have addressed this issue and reported that NOESY cross peaks would be detectable if the population of the folded conformation were at least ~10%. With the possible hydrophobic clustering effect and the observation of a *cis*-peptide bond, structure calculation was carried out.

The three-dimensional solution structures of **1** and **2** in water and chloroform, respectively, have been determined based on NMR data using the program DGII/SA followed by energy

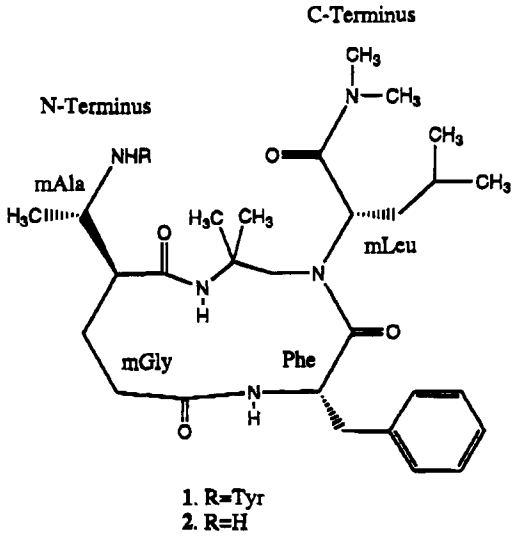

Fig. 1. Chemical structure of 12-membered cyclic enkephalin peptidomimetic. For clarity normal amino-acid convention was used for this peptide mimetic. The 'm' before the three letter code for each amino acid stands for 'mimetic' of that amino-acid. Regardless of the hetero-atom type in the 'mimetic' amino acid, the position of each hetero-atom corresponds to the N, C^α, and C′ hetero-atoms of the normal amino acid.

minimization. Solution conformations of cyclic enkephalin analogues have previously been studied in different solvents by the combined use of molecular mechanics conformational analysis, NOE, and molecular dynamics [20,41–43]. However, to our knowledge, this is one of the first cases where structures of this type and size were calculated in both aqueous and organic solvent. The structures were calculated using torsion angles, distance constraints derived from ROESY experiments, and anti-distance constraints (adc) [32]. In each case, 20 structures were calculated. The total energy for all 20 three-dimensional solution structures determined in water ranged from −28.0 to 29.0 kcal/mol and constraint violation energy of 1.9 to 9.1 kcal/mol. Only one structure had a positive total energy of 29.0 kcal/mol which also had the highest constraint violation energy of 9.1 kcal/mol. In chloroform, the total energy for all 20 structures ranged from −11.8 to 9.0 kcal/mol and constraint violation energy of 2.1 to 6.3 kcal/mol. The structures were selected based on a 20 kcal/mol cutoff of total energy and less than 4.0 kcal/mol constraint violation energy from the lowest energy structure. In total, 14 structures from chloroform and 15 structures from water data were chosen for further analysis. The energies for 14 best three-dimensional solution structures calculated in chloroform range from −11.8 to −1.3 kcal/mol with a mean of −5.8 ± 3.3 and 2.1 to 4.0 kcal/mol with a mean of 2.8 ± 0.7 for total and constraint violation energies, respectively. The energies for the 15 best solution structures in water range from −28.0 to −10.2 kcal/mol with mean of −21.6 ± 5.7 and 1.9 to 3.8 kcal/mol with a mean of 2.7 ± 0.7 for total and constraint violation energies, respectively. The rms deviation was calculated based on all heavy atoms within the cyclic system. In chloroform, the two distinct families exist within the 14 structures with rmsd of 0.23 Å. The two families differ principally in the puckering of the gem-dimethyl group in the linker region (Fig. 2a). The 15 best structures in water with an average rmsd of 0.29 Å are shown in Fig. 2b. All structures in both solvents display a *cis*-peptide bond between the Phe and the C-terminal Leu residue. The use of the gem-dimethyl substitution and length of the linker seems critical for the control of this peptide bond.

In contrast to the more structured side chains of Phe and Leu, the N-terminal Tyr is not structured. This is evident from the lack of inter-residue tyrosine aromatic side chain–side chain interactions. Thus, for the purpose of clarity this residue was not included in the analysis. For structures in both water and chloroform, the side chain dihedral angle (χ_1) of Leu displays a high preference for a χ_1 of −60°. The Phe side chain shows a preference for a χ_1 of +60° in chloroform and a χ_1 of 180° in water. In chloroform, 12 structures occupy χ_1 angle of +60° and two structures with 180°. In water, 14 structures occupy χ_1 of 180° and one structure with χ_1 of −60°. This represents the most notable difference between the structures in water and in chloroform. The observation of more than one conformation for the side chain of Phe in both water and chloroform indicates that there is conformational averaging for this side chain. However, the structures described here represent at least one non-random conformation present in each solvent.

It is rare to observe a χ_1 angle of +60° for a Phe residue in a protein [44–46]. This anomalous observation is presumably due to the effect of chloroform. The χ_1 angle of +60° positions this side chain away from the main body of the molecule and into the solvent. The bulky aromatic side chain is isolated from the other hydrophobic residues and is readily solvated through its interaction with the chloroform solvent. In stark contrast, in water the hydrophobic side chains are clustered together to minimize the unfavorable interaction with the highly polar solvent. This effect can be viewed by comparing the hydrophobic (carbon atoms) and hydrophilic (nitrogen and oxygen atoms) solvent accessible surface area (SASA) [47] of representative chloroform and water structures (Fig. 3a,b) using probe radii of 1.4 Å and 2.4 Å for water and chloroform, respectively. The total hydrophobic SASA is reduced from 846.3 Å^2 in the chloroform structure to 621.3 Å^2 in the water structure, while the

Table 1a
^{1}H NMR assignments of **1** in 90% ^1H_2O/10% ^2H_2O at 5°C[a]

Residue	NH	$C^\alpha H$	$C^\beta H$	Others
Tyr-0		4.10	3.09, 3.03	7.17 ($C^\delta H$), 6.89 ($C^\epsilon H$)
mAla-1[c]	8.33	4.02	1.13	2.24(mCO-H)
mGly-2[c]	1.38	2.05		
Phe-3	8.75	5.02	3.15	7.30 ($C^\delta H$), 7.40 ($C^\epsilon H$), 7.38 ($C^\zeta H$)
mLeu-5[c]		4.66	1.54, 1.43	1.30 ($C^\gamma H$), 0.90 ($C^\delta H$)
C-terminal-NMe's				3.01, 2.88
Linker	10.35	1.43, 1.37 (gem-dimethyl)	4.13, 3.68	

[a] Chemical shifts are referenced to water at 5°C as 4.96 ppm.

Table 1b
^{1}H NMR assignments of **2** in $CDCl_3$ at −10°C[b]

Residue	NH	$C^\alpha H$	$C^\beta H$	Others
mAla-1[c]		3.42	1.32	2.60 (mCO-H)
mGly-2[c]	1.95, 1.84	2.36, 2.22		
Phe-3	7.84	4.80	3.15, 2.97	7.20–7.24 (aromatic protons)
mLeu-4[c]		4.46	1.52, 1.12	1.35($C^\gamma H$); 0.89, 0.79($C^\delta H$)
C-terminal-NMe's			3.01, 2.87	
Linker		1.22, 1.16 (gem-dimethyl)	3.47, 3.02	

[b] Chemical shifts are referenced to residual $CHCl_3$ at −10°C as 7.26 ppm.
[c] The 'm' before the three letter code for each amino acid stands for 'mimetic' of that amino acid. The position of each hetero-atom type in the 'mimetic' amino acid corresponds to the N, C^α, and C′ hetero-atoms of the normal amino acid.

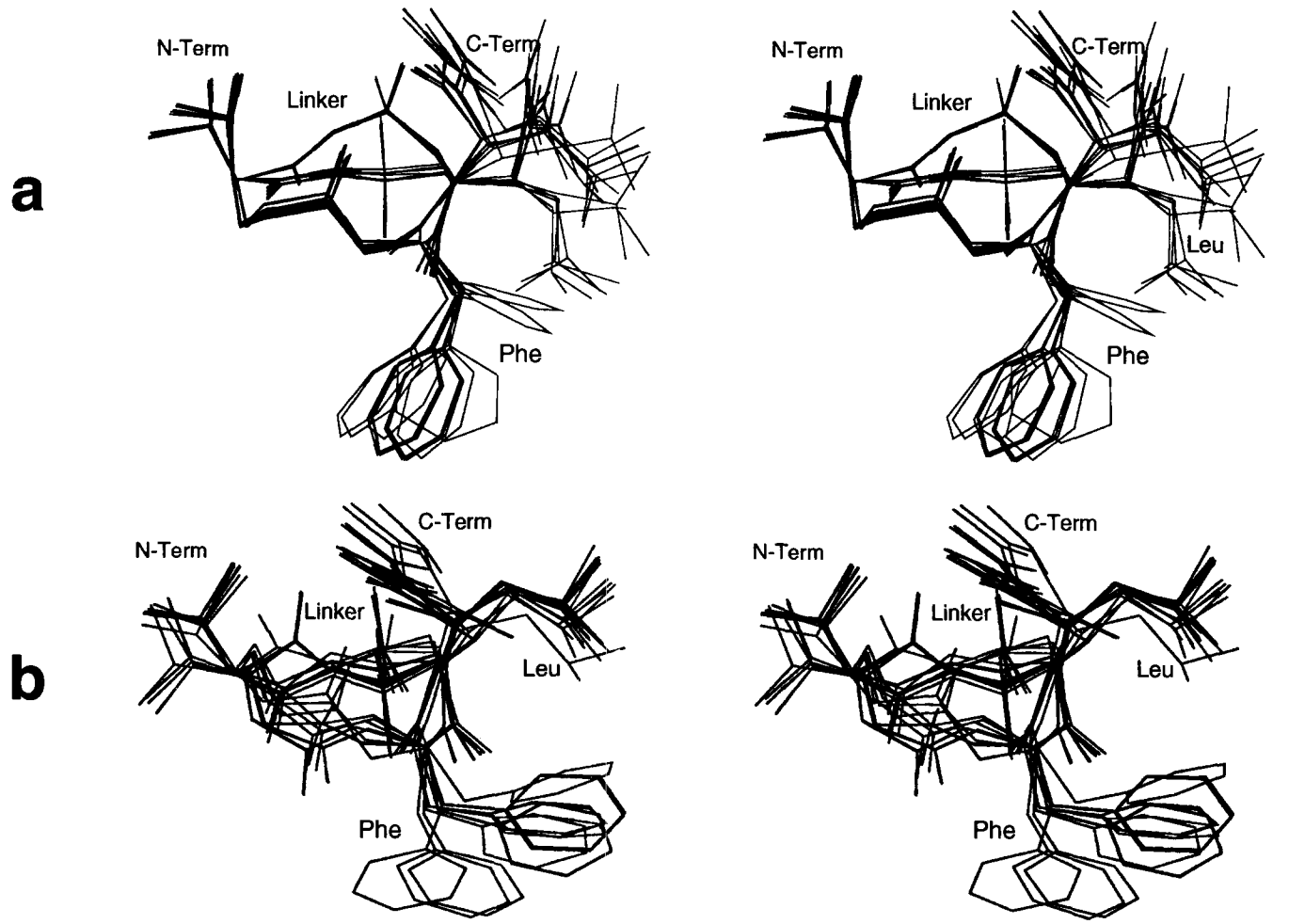

Fig. 2. Stereoview of the solution structures of peptidomimetic (a) in chloroform (magenta) and (b) in water (green). The 14 solution structures in chloroform (top) is shown with gem-dimethyl linker facing the back while the Phe residue is up front pointing down. All 15 structures calculated from water data are shown (bottom) in a similar orientation as the chloroform structures.

total hydrophilic SASA is increased from 77.2 Å^2 in chloroform to 84.8 Å^2 in water. In water, the side chain of the Phe rotates from the 180° to +60° conformation so that the side chains of Phe and Leu, the gem-dimethyl group of the linker, and the C-terminal N-methyls collapse together to form a hydrophobic patch. Concomitantly, this Phe side chain rotation exposes the carbonyl and amide groups of the peptide bond between the mGly and Phe residues (0.6 Å^2 in chloroform to 15.7 Å^2 in water) and carbonyl oxygen of Phe (0.0 Å^2 in chloroform to 4.0 Å^2 in water) to the aqueous environment. A similar observation was made during NMR restrained molecular dynamic simulations of the cyclic octapeptide hymenistatin 1 in chloroform and DMSO solutions [15]. The SASA of the carbonyl oxygen at Pro-5 of hymenistatin 1 was reduced in DMSO (1.6 Å^2 in DMSO compared to 5.2 Å^2 in chloroform). In contrast, the amide nitrogen of Leu-6 which was completely buried in chloroform became exposed in DMSO due to a favorable H-bond interaction in this solvent.

4. Conclusions

We have determined the three-dimensional solution structure of a 12-membered constrained peptidomimetic in both chloroform and water. Key structural feature of this cyclic mimetic include the solvent independent *cis*-peptide bond which is controlled by the linker and the formation of a hydrophobic patch in water. The hydrophobic clustering observed in water may well represent an accurate description of the conformational effects induced on peptides by bulk polar solvent. A similar conclusion was derived through the computer simulation study of a cyclic hexapeptide that displayed a hydrophobic clustering between the Phe and Leu residues as a key structural driving force [48]. Statistical analysis of residue associations in protein structures have shown a high propensity for interactions between Leu and Phe residues [49,50]. Moreover, Kelley and co-workers have implicated hydrophobic clustering as a necessary event in β-sheet nucleation from their mimetic framework [51]. These observations are also consistent with the view of hydrophobic collapse as a dominant force in protein folding [52]. The effect of environment, hydrophobic clustering, and surface hydrophobicity have all been shown to be important factors in conformation, nucleation, protein folding, and protein–ligand interactions [15,19,39,40,48,51–59]. We have directly demonstrated that the environment plays a critical role

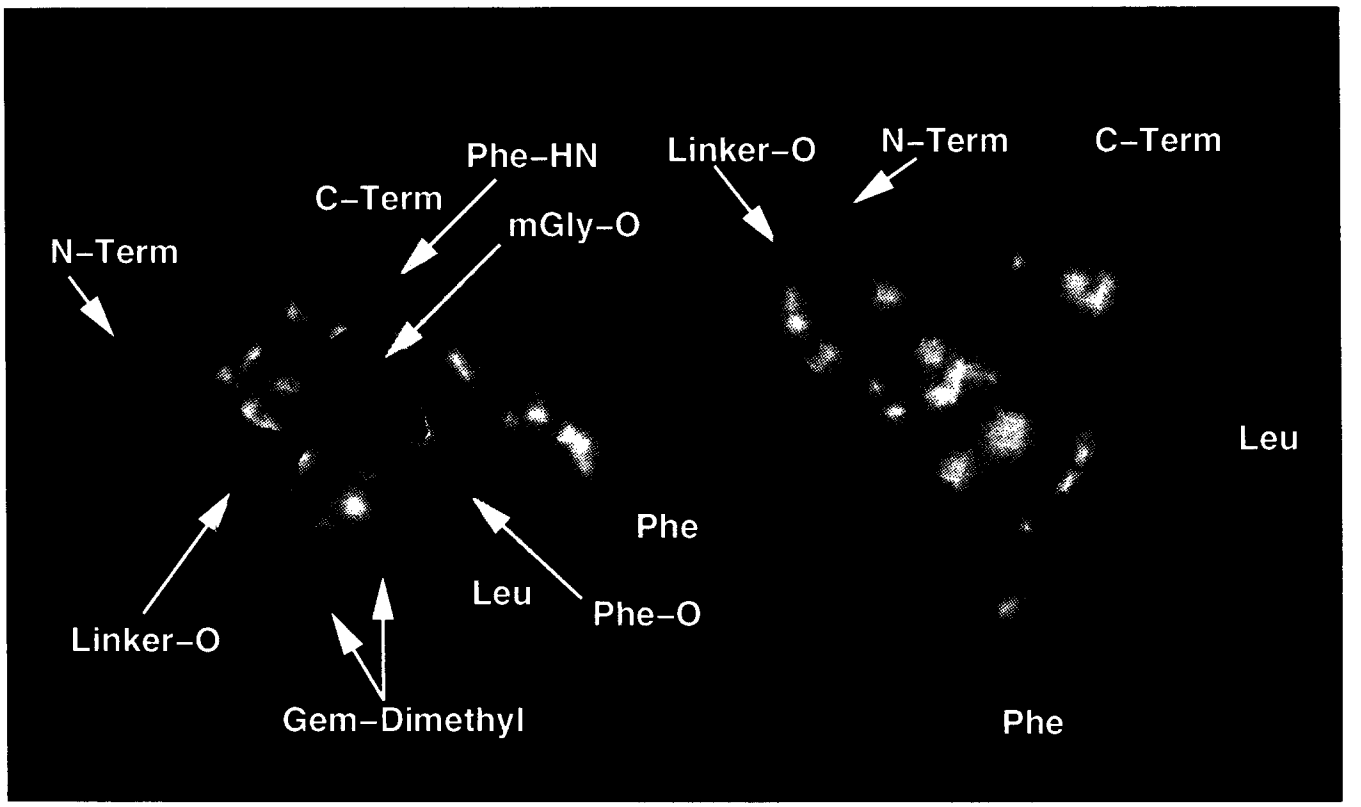

Fig. 3. View of the solvent accessible surface area of structure (a) in water and (b) in chloroform with hydrophobic surface in gray and hydrophilic surface in red. The structure in water shows scattered patches of hydrophilic surface area exposed to the environment in order to maximize hydrogen bond interaction with solvent, water. In contrast, in chloroform there is only one strip of hydrophilic surface area. Side chains of Leu, Phe, and gem-dimethyl groups form a compact hydrophobic surface in water while in chloroform, the side chain of Phe protrudes out and is exposed to solvent.

in conformational and structural aspects of even highly constrained molecules in solution.

Acknowledgments: We gratefully acknowledge the generous financial support of the Camille and Henry Dreyfus Foundation (M.K.), and the assistance of Kathy Hjelmeland and Melody Ferguson in the preparation of this manuscript. M.K. is an Established Investigator of the American Heart Association.

References

[1] Greer, J., Erickson, J.W., Baldwin, J.J. and Varney, M.D. (1994) J. Med. Chem. 37, 1035–1054.
[2] Kahn, M. (1993) SYNLETT, 821–826.
[3] Olson, G.L. et al. (1993) J. Med. Chem. 36, 3039–3049.
[4] Wiley, R.A. and Rich, D.H. (1993) Med. Res. Rev. 13, 327–384.
[5] Giannis, A. and Kolter, T. (1993) Angew. Chem. Int. Ed. Engl. 32, 1244–1267.
[6] Nikiforovich, G.V., Kao, J.L.-F., Plucinska, K., Zhang, W.J. and Marshall, G.R. (1994) Biochemistry 33, 3591–3598.
[7] Bach, A.C.I., Eyermann, C.J., Gross, J.D., Bower, M.J., Harlow, R., Weber, P.C. and DeGrado, W.F. (1994) J. Am. Chem. Soc. 116, 3207–3219.
[8] Bartosz-Bechowski, H., Davis, P., Zalewska, T., Slaninova, J., Porreca, F., Yamamura, H.I. and Hruby, V.J. (1994) J. Med. Chem. 37, 146–150.
[9] Barrow, C.J., Doleman, M.S., Bobko, M.A. and Cooper, R. (1994) J. Med. Chem. 37, 356–363.
[10] Ali, F.E. et al. (1994) J. Med. Chem. 37, 769–780.
[11] Smythe, M.L. and von Itzstein, M. (1994) J. Am. Chem. Soc. 116, 2725–2733.
[12] Fujikawa, A. et al. (1994) J. Org. Chem. 59, 570–578.
[13] Jackson, S. et al. (1994) J. Am. Chem. Soc. 116, 3220–3230.
[14] Lomize, A.L., Flippen-Anderson, J.L., George, C. and Mosberg, H.I. (1994) J. Am. Chem. Soc. 116, 429–436.
[15] Konat, R.K., Mierke, D.F., Kessler, H., Kutscher, B., Bernd, M. and Voegeli, R. (1993) Helv. Chim. Acta 76, 1649–1666.
[16] Matsunaga, T.O., Collins, N., Ramaswami, V., Yamamura, S.H., O'Brien, D.F. and Hruby, V.J. (1993) Biochemistry 32, 13180–13189.
[17] Bienstock, R.J., Rizo, J., Koerber, S.C., Rivier, J.E., Hagler, A.T. and Gierasch, L.M. (1993) J. Med. Chem. 36, 3265–3273.
[18] Polinsky, A., Cooney, M.G., Toy-Palmer, A., Ösapay, G. and Goodman, M. (1992) J. Med. Chem. 35, 4185–4194.
[19] Köck, M., Kessler, H., Seebach, D. and Thaler, A. (1992) J. Am. Chem. Soc. 114, 2676–2686.
[20] Hruby, V.J., Kao, L.-F., Pettitt, B.M. and Karplus, M. (1988) J. Am. Chem. Soc. 110, 3351–3359.
[21] Gardner, B., Nakanishi, H. and Kahn, M. (1993) Tetrahedron 49, 3433–3448.
[22] Hughes, J., Smith, T.W., Kosterlitz, H.W., Fothergill, L.A., Morgan, B.A. and Morris, H.R. (1975) Nature 258, 577–579.
[23] Rance, M., Sorensen, O.W., Bodenhausen, G., Wagner, G., Ernst, R.R. and Wüthrich, K. (1983) Biochem. Biophys. Res. Commun. 117, 479–485.
[24] Kessler, H., Griesinger, C., Kerssebaum, R., Wagner, K. and Ernst, R.R. (1987) J. Am. Chem. Soc. 109, 607–609.
[25] Jeener, J., Meier, B.H., Bachmann, P. and Ernst, R.R. (1979) J. Chem. Phys. 71, 4546–4553.
[26] Bax, A., Sklenar, V., Clore, G.M. and Gronenborn, A.M. (1987) J. Am. Chem. Soc. 109, 6511–6513.
[27] States, D.J., Habekorn, R.A. and Ruben, D.J. (1982) J. Magn. Reson. 48, 286–292.
[28] Marion, D. and Wüthrich, K. (1983) Biochem. Biophys. Res. Commun. 113, 967–974.
[29] Pardi, A., Billeter, M. and Wüthrich, K. (1984) J. Mol. Biol. 180, 741–751.

[30] Nagayama, K. and Wüthrich, K. (1981) Eur. J. Biochem. 115, 653–657.
[31] Wüthrich, K., Billeter, M. and Braun, W. (1983) J. Mol. Biol. 169, 949–961.
[32] Brüschweiler, R.P., Blackledge, M. and Ernst, R.R. (1991) J. Biomol. NMR 1, 3–11.
[33] Wüthrich, K. (1986) NMR of Proteins and Nucleic Acids, Wiley, New York.
[34] Ramurthy, S., Lee, M.S., Nakanishi, H., Shen, R. and Kahn, M. (1994) Bioorg. Med. Chem. 2, 1007–1013.
[35] Nakanishi, H., Chrusciel, R.A., Shen, R., Bertenshaw, S., Johnson, M.E., Rydel, T.J., Tulinsky, A. and Kahn, M. (1992) Proc. Natl. Acad. Sci. USA 89, 1705–9.
[36] Chen, S. et al. (1992) Proc. Natl. Acad. Sci. USA 89, 5872–5876.
[37] Bundi, A. and Wüthrich, K. (1979) Biopolymers 18, 285–297.
[38] Neri, D., Wider, G. and Wüthrich, K. (1992) Proc. Natl. Acad. Sci. 89, 4397–4401.
[39] Neri, D., Billeter, M., Wider, G. and Wüthrich, K. (1992) Science 257, 1559–1563.
[40] Lumb, K.J. and Kim, P.S. (1994) J. Mol. Biol. 236, 412–420.
[41] Graham, W.H., Carter, E.S., II and Hicks, R.P. (1992) Biopolymers 32, 1755.
[42] Mierke, D., Said-Nejad, O.E., Schiller, P.W. and Goodman, M. (1990) Biopolymers 29, 179–196.
[43] Schmidt, R., Vogel, D., Mrestani-Klaus, C., Brandt, W., Neubert, K., Chung, N.N., Lemieux, C. and Schiller, P.W. (1994) J. Med. Chem. 37, 1136–1144.
[44] Abagyan, R.A. and Totrov, M. (1994) J. Mol. Biol. 235, 983–1002.
[45] Blaber, M., Zhang, X.-J., Lindstrom, J.D., Pepiot, S.D., Baase, W.A. and Matthews, B.W. (1994) J. Mol. Biol. 235, 600–624.
[46] Schrauber, H., Eisenhaber, F. and Argos, P. (1993) J. Mol. Biol. 230, 592–612.
[47] Lee, B. and Richards, F.M. (1971) J. Mol. Biol. 55, 379–400.
[48] Simmerling, C. and Elber, R. (1994) J. Am. Chem. Soc. 116, 2534–2547.
[49] Karlin, S., Zuker, M. and Brocchieri, L. (1994) J. Mol. Biol. 239, 227–248.
[50] Singh, J. and Thornton, J.M. (1992), Vol. 2, pp. 428–827 IRL Press, New York.
[51] Tsang, K.Y., Diaz, H., Graciani, N. and Kelly, J.W. (1994) J. Am. Chem. Soc. 116, 3988–4005.
[52] Dill, K.A. (1990) Biochemistry 31, 7133–7155.
[53] Waterhous, D.V. and Johnson, W.C.J. (1994) Biochemistry 33, 2121–2128.
[54] Young, L., Jernigan, R.L. and Covell, D.G. (1994) Protein Science 3, 717–729.
[55] Lee, B. (1993) Protein Science 2, 733–738.
[56] Eriksson, A.E., Baase, W.A., Zhang, X.-J., Heinz, D.W., Blaber, M., Baldwin, E.P. and Matthews, B.W. (1992) Science 255, 178–183.
[57] Weber, C., Wider, G., von Freyberg, B., Traber, R., Braun, W., Widmer, H. and Wüthrich, K. (1991) Biochemistry 30, 6563–6574.
[58] Evans, P.A., Topping, K.D., Woolfson, D.N. and Dobson, C.M. (1991) Proteins: Struct. Func. Genet. 9, 248–266.
[59] Wright, P.E., Dyson, H.J. and Lerner, R.A. (1988) Biochemistry 27, 7167–7175.